Nitrogen-doped graphic carbon protected Cu/Co/CoO nanoparticles for ultrasensitive and stable non-enzymatic determination of glucose and fructose in wine

Juan He[a,b,c], Yijun Zhong[d], Qing Xu[e], Hainan Sun[a,b,c], Wei Zhou[a,b,c], and Zongping Shao[a,b,d]**

[a] Jiangsu National Synergetic Innovation Center for Advanced Materials (SICAM), No. 5 Xinmofan Road, Nanjing 210009, P.R. China

[b] State Key Laboratory of Materials-Oriented Chemical Engineering, Nanjing Tech University, No. 5 Xinmofan Road, Nanjing 210009, P.R. China

[c] College of Chemical Engineering, Nanjing Tech University, No. 5 Xinmofan Road, Nanjing 210009, P.R. China

[d] Department of Chemical Engineering, Curtin University, Perth, Western Australia 6845, Australia

[e] School of pharmaceutical sciences, Nanjing Tech University, No.30 Puzhunan Road, Nanjing 210009, P.R. China

*Corresponding author at: E-mail addresses: zhouwei1982/njtech.edu.cn (W. Zhou) and shaozp/njtech.edu.cn (Z. Shao)

Keywords: Nitrogen-doped graphic carbons; Cu/Co/CoO nanoparticles; Synergistic effect; glucose and fructose; Screen-printed carbon electrodes; wine

Abstract: Food safety has always been a very serious and global concern. Content determination of each component is one of the most routine analyses in food testing. Here, nitrogen-doped graphic carbon (NGC)-coated Cu/Co/CoO nanoparticles (Cu/Co/CoO/NGC) show excellent performance for glucose and fructose detection in wine. The high sensitivity (1,035 μA mM^{-1} cm^{-2}), low determination (0.2 μM) and large linear range (10-9,300 μM) characteristic of the Cu/Co/CoO/NGC sensor are attributed to the synergistic effect between the Cu, Co and CoO nanoparticles coated by NGC and the catalytically active M-Nx moieties (M=Cu and Co). Importantly, the good stability and antioxidation of the Cu/Co/CoO/NGC electrode result from the protection provided by the NGC shell. In addition, disposable, low-cost, and compact screen-printed carbon electrodes (SPCEs) modified by the Cu/Co/CoO/NGC (Cu/Co/CoO/NGC/SPCEs) were used to detect the sugar content in wine samples with a good reliability (R.S.D.=1.7%) and recovery (103.2%). Thus, Cu/Co/CoO/NGC/SPCEs will be popular in the detection of real samples.

1. Introduction

Human consumption level is constantly increasing with the continuous development of the world economy. Wine as a fashionable, healthy, and low-alcohol-content beverage is popular with numerous consumers. Its sales are increasing rapidly, especially in new world markets such as China Thorpe.[1] Therefore, detailed quality identification and component detection in wine during the making and storage processes are essential.[2]

Sugar (glucose and fructose) is both a source for fermentation yeast, and the substrate that limits yeast growth.[3] Hence, the amount of sugar fermented affects the content of ethanol, and the non-fermented sugar determines the sweetness of the wine. However, traditional methods for sugar detection are time-consuming and expensive, and they require complex operating procedures and specialized experimental instruments, such as mass spectrometry and high-performance liquid chromatography (HPLC). Therefore, a rapid, simple and reliable electrochemical sensor for sugar is in high demand.[4, 5] Non-enzymatic electrochemical sensors have great practical applications due to their high sensitivity, long-term stability and convenience for storage.[6]

The various electrocatalytic materials for electrode modification have been widely studied by researchers. Although the previous noble metals (Pt, Au, Pd and their alloys) show great electroactivity, their practical commercial application is limited by their high cost and limited reserves.[7, 8] Consequently, the pursuit of alternatives materials with nonprecious metal catalysts has become a hot topic in the field of catalysis. Recently, the transition metal oxides, such as NiOx, CuOx, and CoOx, have gained more interested because of their low cost and good sensing performance for glucose.[6-9] Their stability, however, is still not satisfied under harsh conditions due to the direct contact of the metals with reactants and the reaction media.

Herein, a promising strategy to form a core-shell structure between a thin layer of carbon materials (graphene and graphic carbon) and nonprecious metal or metallic oxides has exhibited excellent advantages towards catalysis. For example, Liu et al. prepared transition metal nanoparticles (Fe, Co, and Ni) coated with N-doped graphene shells, where encapsulated Co showed a higher activity for oxygen reduction reaction (ORR).[10] Noh et al. demonstrated that Cu particles coated with N-doped carbon (Cu/N-C) displayed dramatically improved ORR activity comparable to

the Pt/C catalyst and a better stability than Pt/C under long-term detection.[11] Chen et al. prepared carbon-coated Cu-Co bimetallic nanoparticales by a solvothermal method for the production of the biofuel 2,5-dimethylfuran.[12] In addition, extensive applications for this kind of structure include fuel cells, water splitting, CO_2 conversion, solar cells, and metal-air batteries.[13] Such structured catalysts have also revealed considerable superiority towards the reaction system of glucose sensing detection owing to the synergistic effect between the carbon shells and the core metallic nanoparticles.

In our work, nitrogen-doped graphic carbon (NGC)-coated Cu/Co/CoO nanoparticles (Cu/Co/CoO/NGC) show higher sensitivity and electrocatalytic activity for the determination of glucose and fructose compared to NGC-coated copper nanoparticles (Cu/NGC), and NGC-coated cobalt/cobalt oxide nanoparticles (Co/CoO/NGC). The sensitivity, limit of detection and linear range of Cu/Co/CoO/NGC towards surge solution are 1,035 μA mM^{-1} cm^{-2}, 0.2 μM and 10-9,300 μM, respectively. Here, we studied the synergistic effect between NGC-coated Cu, Co and CoO nanoparticles by a series of controlled tests. In addition, we demonstrated that the closed NGC layers effectively protect the metallic nanoparticles from oxidation and destruction in harsh conditions, leading to good stability. In addition, the Cu/Co/CoO/NGC/SPCEs sensor (screen-printed carbon electrodes modified by Cu/Co/CoO/NGC) shows excellent performance for glucose and fructose detection. Cu/Co/CoO/NGC/SPCEs was used to detect the content of sugar in wine with low cost and high reproducibility (R.S.D. < 4%). In fact, SPCEs are one of the most promising sensors towards real sample applications with the advantages of high versatility, rapid processing, and low cost.

2. Experimental

2.1. Materials

Melamine and D(+)-glucosamine hydrochloride (GAH) were purchased from Sinopharm Group Chemical Reagent. $Co(NO_3)_2 \cdot 6H_2O$, $Cu(NO_3)_2 \cdot 3H_2O$, and ethylenediaminetetraacetic acid (EDTA) were purchased from Sinopharm Group Chemical Reagent. The ammonia solution (28% in NH_3 in H_2O) was purchased from Shanghai Lingfeng Chemical Reagent. Ar (99.999%) gas cylinders were purchased

from Nanjing Shangyuan. All reagents were of analytical grade. All solutions were prepared with de-ionized water. Screen-printed carbon electrode (SPCE) equipment with a three-electrode layout was purchased from Shanghai Molybdenum Electronics Technology Co., Ltd. Wine (yellow tail merlot, Demi sec, 13.5% vol wine accuracy) was purchased from Casella private wine Co., Ltd.

2.2. Synthesis of Cu/Co/CoO/NGC

First, 40 g of melamine and 1 g of GAH were mixed with 350 mL of deionized water and stirred vigorously. Then, 0.95 g of $Co(NO_3)_2 \cdot 6H_2O$, 0.95 g of $Cu(NO_3)_2 \cdot 3H_2O$ (the molar ratio of Cu:Co is 1:1), and 0.48 g of EDTA were put into 50 mL of deionized water with the addition 3-5 mL an ammonia solution dropwise to form a transparent solution. Then, the transparent solution was mixed with the above solution and stirred in a 60-70 °C oil bath until a solid mixture was formed. Finally, the ground mixture powder was calcined at 600 °C for 1 h followed by another calcination at 800 °C for 1 h in Ar atmosphere, and the heating rate was 2.5 °C min^{-1}.

2.3. Synthesis of Cu/NGC, Co/CoO/NGC, and Cu/Co/CoO/GC

Cu/NGC, Co/CoO/NGC, and Cu/Co/CoO/GC were obtained via a similar procedure to the Cu/Co/CoO/NGC, except that 0.95 g of $Cu(NO_3)_2 \cdot 3H_2O$ replaced 0.95 g of $Co(NO_3)_2 \cdot 6H_2O$ for Cu/NGC, while 0.95 g of Co/CoO/NGC replaced 0.95 g of $Cu(NO_3)_2 \cdot 3H_2O$ for Co/NGC. The Cu/Co/CoO/GC which did not include the nitrogen resources of EDTA and $NH_3 \cdot H_2O$. The catalysts of Cu/NGC and Co/CoO/NGC contain equimolar amounts of metal ions.

2.4. Characterizations

The constituent phase of Cu/Co/CoO/NGC, Cu/NGC, and Co/CoO/NGC was characterized by room-temperature powder X-ray diffraction (XRD, Rigaku Smartlab 3 kW) with filtered Cu Kα radiation (λ = 1.5406 Å) operated at a tube voltage of 40 kV and a current of 40 mA. The scanning range was from a 2θ of 10 ° to 80 ° with a scan rate of 10 ° min^{-1}.

The microstructure of Cu/Co/CoO/NGC, Cu/NGC, and Co/CoO/NGC was obtained by a field-emission scanning electron microscope (FE-SEM, Hitachi S-4800) operated at 5 kV.

The surface area and pore size distribution of Cu/Co/CoO/NGC, Cu/NGC, and Co/CoO/NGC were measured by nitrogen adsorption-desorption tests (BELSOR-MAX). The analysis results were calculated using the Brunauer-Emmett-Teller (BET) and Barret-Joyner-Halenda (BJH) methods. Approximately 0.1 g of the powders was degassed at 200 °C for 2.5 h before the N_2-adsorption measurement at liquid nitrogen temperature (77 K).

The X-ray photoelectron spectroscopy (XPS, PHI5000 VersaProbe) equipped with an Al Kα X-ray source was used to obtain the materials of the surface chemical species and their relative amounts. All binding energies were calibrated to the C1s binding energy of adventitious carbon at 284.8 eV. The data were fitted by the public software package XPSPEAK.

High-resolution transmission electron microscopy (HR-TEM) images and the corresponding energy-dispersive X-ray spectroscopy (EDX) mapping images were taken on a field-emission transmission electron microscope (FEI Tecnai G2F30 S-TWIN) operated at 300 kV.

High-performance liquid chromatography (HPLC, Shimadzu Corporation) was equipped with a 4.6 mm×250 mm steel carbohydrate cartridge column (Sepax Hp-Amino). The filled mobile phase was a solution mixture of acetonitrile and water (75:25). The flow rate was 1 mL min^{-1} with a column at 30 °C. The peaks of glucose and fructose in wine samples were detected by a refractive index detector (Shimadzu Corporation), and were determined based on standard samples of glucose and fructose. The concentrations were also calculated according to the standard curve using the calibration characteristic.

2.5. Preparation of catalyst inks, modified electrodes, and electrochemical tests

First, 20 mg of catalysts (Cu/Co/CoO/NGC, Cu/NGC, and Co/CoO/NGC) and 0.1 mL of a 0.5 wt.% Nafion solution were mixed with 0.9 mL of ethanol. The mixture solutions were then subjected to sonication to obtain a homogeneous catalyst ink. For each catalyst case, 5 μL of ink was dropped on the surface of the glassy carbon electrode (GCE, the surface area of the electrode was 0.196 cm^2) and dried at room temperature for at least 30 min to prepare the available modified GCE sensor. Prior to modification, GCE was polished by 0.05 μm alumina powder, and then ultrasonically cleaned in de-ionized water and ethanol.

Screen-printed carbon electrodes (SPCEs) are a three-electrode configuration (working, counter and reference electrodes) printed on the plastic substrates. The working and counter electrodes were printed using graphite ink and the reference electrode was formed using Ag/AgCl ink. The surface area of the working electrode is 0.07 cm^2. To form a modified SPCE sensor (Cu/Co/CoO/NGC/SPCE), 3 μL of Cu/Co/CoO/NGC catalyst ink was dropped on the surface of the working field.

All electrochemical tests were carried out using a CHI 760E electrochemical workstation (Shanghai Chenhua Co. Ltd., China). A standard three-electrode electrochemical installation (Pine Research Instrumentation) was used for the electrochemical measurements. For the experimental studies, the working electrode was a catalyst-modified GCE or SPCEs, the reference electrode was an Ag|AgCl (3.5 M KCl), and the counter electrode was a platinum wire.

3. Results and Discussion

3.1. Characterization of catalysts

The Cu/Co/CoO/NGC was prepared using a soft-template method, where melamine acts as the soft template during the in situ synthesis of NGC. The GAH, EDTA, cobalt nitrate and copper nitrate act as the carbon, nitrogen, cobalt and copper sources, respectively. As shown in Figure 1, the coated Cu/Co/CoO nanoparticles with a diameter of ~20 nm were homogeneously distributed and anchored on the NGC layers. In addition, the NGC shells over the metallic nanoparticles were clear and in the size range from 25 to 30 nm (Figure 1C). There is a synergistic effect between the NGC and metallic nanoparticles, which not only improves the conductivity and the catalytic activity of metallic nanoparticles but also prevents the aggregation in the NGC layers to retain the high surface area and pore volume.[14] More importantly, the stability of the coated metallic nanoparticles is enhanced observably because of the protection provided by the NGC shell. Mostly, our electrochemical tests were performed in stirred alkali solution. Therefore, this core-shell structure of the catalysts greatly benefits the service life of the catalyst.

To investigate the elemental composition and distribution of the Cu/Co/CoO/NGC, energy-dispersive spectroscopy (EDS) elemental mapping analysis was conducted in the marked areas (Figure S1). The round metal nanoparticles contained both Co and Cu. As shown in the enlarged areas of Figure 1C (areas 1, 2,

and 3), the lattice fringe spacing of 2.046, 2.086 and 2.118 Å corresponds to the (111) plane of Co, the (111) plane of Cu and the (200) plane of CoO, respectively. Figure 1C (area 4) shows that the thickness of the carbon shells is approximately 2.3 nm.

Electrochemical impedance spectroscopy (EIS) was used to perform the interface properties of different modified electrodes. Figure S2 shows the Nyquist diagrams of the Cu/Co/CoO/NGC, Co/CoO/NGC, Cu/NGC, O-Cu/Co/CoO/NGC, and R-Cu/Co/CoO/NGC electrodes in 0.2 M NaOH solution over a frequency range of 0.1-100,000 Hz. The semicircle portion represents the charge transfer resistance, and the smallest half cycle has the smallest resistance value. Therefore, upon looking at Figure S2, The semicircle size decreases in the order of Cu/Co/CoO/NGC > O-Cu/Co/CoO/NGC > Cu/NGC > R-Cu/Co/CoO/NGC > Co/CoO/NGC > bare electrode, which reflects that the Cu/Co/CoO/NGC electrode has the lowest resistance value while the bare electrode has the highest value, indicating that the catalysts were actually adhered to the surface of electrodes and reduced the charge transfer resistance at electrode interface.

The XRD patterns (Figure S3) reflect the predominant structures of metal and metal oxides, such as the Cu, Co and CoO. The peaks of Co and CoO at approximately 36.4 °, 42.3 °, and 44.1 ° for Cu/Co/CoO/NGC slightly shifted to a low angle compared with the Cu/NGC and Co/CoO/NGC samples. XRD patterns for the reduction and oxidation samples (R-Cu/Co/CoO/NGC and O-Cu/Co/CoO/NGC treated in a 10% H_2/Ar atmosphere at 800 °C for 4 h and in air at 250 °C for 24 h, respectively) are shown in Figure S3. The peak of CoO for R-Cu/Co/CoO/NGC at approximately 36.4 ° could also be observed in the pattern, suggesting that the metal oxide (CoO) in the Cu/Co/CoO/NGC sample was not completely reduced to metal element (Co) in the reducing conditions. The unchanged structure of O-Cu/Co/CoO/NGC proves that the core-shell structure of the graphic carbon-coated metal element has superior antioxidation ability.

X-ray photoelectron spectroscopy (XPS) is used to determine the surface composition of the catalysts. The fitted N 1s spectra (Figure 2a-c, and detailed fitted data in Table S1) prove the presence of prophyrin-like metal-coordinated M-Nx moieties (399.7 eV), pyridinic N (398.8 eV), pyrrolic N (400.9 eV), graphitic N (402.9 eV), and oxidized N (405.1 eV).[15] The N 1s spectra of all samples are dominated by pyridinic N, and the proportion of M-Nx moiety was the greatest for the

Co/CoO/NGC sample. The detailed information of the Co 2p and Cu 2p spectra for Cu/Co/CoO/NGC, Cu/NGC, and Co/CoO/NGC are presented in Figure S4 and Table S2. For Co 2p, the higher energy band at 795.5 eV and the lower energy band at 780.1 eV are the two distinct energy band profiles for Co 2p3/2 and Co 2p1/2, respectively. CoO and Co-Nx near the surface of the Cu/Co/CoO/NGC and Co/CoO/NGC samples were confirmed by the presence of the Co^{2+} (at approximately 782.8 eV and 798.6 eV) and Co^{3+} (at approximately 780.1 eV and 795.4 eV). Notably, the high oxidation state Cu^{2+} (at approximately 934.6 and 954.7 eV of Cu 2p3/2 and Cu 2p1/2, respectively) was found in the form of Cu-Nx moieties near the surface of the Cu/Co/CoO/NGC and Cu/NGC catalysts.

According to the N_2 sorption isotherms and pore size distribution, the specific surface areas (BET) of Cu/Co/CoO/NGC, Cu/NGC, and Co/CoO/NGC (Figure 2d, Figure S5, and Figure S6), were 159.8, 57.3, and 113.9 $m^2\ g^{-1}$, respectively. All samples exhibited the isotherm characteristic of mesoporous materials (type IV isotherm), featuring hysteresis between the adsorption and desorption profiles. The high specific surface area and presence of meso and/or macropores have been proved beneficial to increase the active sites and promote mass transport on the surface of the materials. The larger specific surface areas and pore size values of Cu/Co/CoO/NGC can be ascribed to inhibited aggregation of the NGC nanosheets due to the metal nanoparticles. The similar specific surface areas and pore sizes of the Cu/Co/CoO/NGC and Co/CoO/NGC samples suggest that the better electrocatalytic activity (in the next section) of Cu/Co/CoO/NGC towards glucose and fructose was not affected by the surface area.

3.2. Catalytic activity towards glucose and fructose

To evaluate the catalytic activity towards glucose and fructose, cyclic voltammetry (CV) between -0.8-0.6 V versus Ag|AgCl (3.5 M KCl) in an Ar-saturated 0.2 M NaOH solution was initially performed in the presence or absence of sugar (5 mM glucose and 5 mM fructose) at a scan rate of 50 mV s^{-1} (Figure 3). An obvious advantage in the oxidation current at approximately 0.4 V for Cu/Co/CoO/NGC compared with the Cu/NGC and Co/CoO/NGC correlates with the synergistic effect between the Cu, Co/CoO nanoparticles coated by NGC.

To determine the electrocatalytically active sites in Cu/Co/CoO/NGC for sugar detection, controlled tests of NGC (without metal elements), R-Cu/Co/CoO/NGC (reduced Cu/Co/CoO/NGC treated in 10% H_2/Ar atmosphere at 800 °C for 4 h), O-Cu/Co/CoO/NGC (oxidized Cu/Co/CoO/NGC treated in air at 250 °C for 24 h), and Cu/Co/CoO/GC which did not include the nitrogen resources of EDTA and $NH_3 \cdot H_2O$ were measured by CV (Figure S7 and S8 (a)) and XRD. For the CV tests, the electrocatalytic activity of R-Cu/Co/CoO/NGC showed a dramatic decrease, while the activity of O-Cu/Co/CoO/NGC remained high towards sugar oxidation compared with Cu/Co/CoO/NGC. Those controlled tests confirm that the active sites of Cu/Co/CoO/NGC for fructose are not metallic Co and Cu but a Cu/Co/CoO hybrid.

From the CV profiles (Figure 3 and Figure S7), three pairs of redox peaks can be assumed, as shown in equations (3-5). The peak pair of A (anodic peak) and A′ (cathodic peak) of Cu/Co/CoO/NGC, Cu/NGC, and R-Cu/Co/CoO/NGC are attributed to the redox reaction between $Cu(OH)_2$ and CuOOH in the alkali solution.[16] The weak peaks at B and B′ of Co/CoO/NGC and R-Cu/Co/CoO/NGC are from the redox reaction between $CoO/Co(OH)_2$ and CoOOH. In addition, the peaks at C and C′ correspond to the reversible reaction between CoOOH and CoO_2.[17, 18] Importantly, the oxidation current at approximately 0.4 V increased significantly in the presence of sugar (a mixed solution of glucose and fructose) for all samples because glucose reacts with catalytic species, such as CuOOH and CoO_2, or with active M-Nx moieties (equations 6 and 7, and Figure 4). Besides, the constant potential chronoamperometry was performed by varying the potential (in 0.1 V step) of the Cu/Co/CoO/NGC electrode between 0.2 and 0.6 V. The steady anodic current increases gradually with the increase of the potential. However, as a high potential would oxidize some interfering species that were stable under relatively low potential, thus 0.4 V was selected the optimal potential (Figure S9).

$$Cu + 2OH^- \leftrightarrow Cu(OH)_2 + 2e \quad (1)$$

$$Co + 2OH^- \leftrightarrow Co(OH)_2 + 2e \quad (2)$$

Peak A/A′: $Cu(OH)_2 + OH^- \leftrightarrow CuOOH + H_2O + e$ (3)

Peak B/B′: $CoO/Co(OH)_2 + OH^- \leftrightarrow CoOOH + H_2O + e$ (4)

Peak C/C′: $CoOOH + OH^- \leftrightarrow CoO_2 + H_2O + e$ (5)

Then, glucose is oxidized to gluconolactone by CuOOH and CoO_2 species as follows:

$$2CuOOH + glucose \leftrightarrow 2Cu(OH)_2 + gluconolactone \quad (6)$$

$$2CoO_2 + glucose \leftrightarrow 2CoOOH + gluconolactone \quad (7)$$

Noticeably, once fructose is mixed with OH^-, it is immediately isomerized and forms the enediol structure. Subsequently, enediol produces glucose and mannose with OH^- (as shown in equation 8).[19, 20] Here, the M-N_4 site is a reasonable single active model compared to other M-Nx functionalities because Busch and Liu et al. calculated the metal as the key affecting the OER and ORR. According to the oxidation process and density function theory (DFT) calculations for the OER, [15-21] we also provide a possible catalytic reaction mechanism for glucose and the M-N_4 active site in alkaline electrolyte (Figure 4). *-OH, *=O, and *-OOH (the binding sites of M-N_4 are denoted as *) are the different intermediates during the oxidation process.

$$fructose + OH^- \leftrightarrow enediol\ anion + OH^- \leftrightarrow glucose + mannose \quad (8)$$

The amperometric method (I-t) was chosen to detect the sensing performance. This test was performed by fixing the potential at the oxidation peak potential value (determined previously from CV measurement) between the catalysis and analyte (0.4 V). Figure 5a shows the current response with the successive addition of the sugar solution (the mixed sugar solution contains an equimolar concentration of glucose and fructose because the concentration is similar to that of the real wine samples) to obtain an increasing concentration from 0.5 μM to 12 mM in a 0.2 M NaOH solution. I-t tests of all modified electrode sensors were performed at least 5 times in a solution stirred at 300 rpm. When the sugar solution was added into the 0.2 M NaOH solution, the current responses of the Cu/Co/CoO/NGC, Cu/NGC, and Co/CoO/NGC electrodes changed rapidly and reached a stable current within 3, 4, and 4 s, respectively. Figures 5b-d, in turn, present the linear fitting results of Cu/Co/CoO/NGC, Cu/NGC, and Co/CoO/NGC between the current response and the sugar concentration. The calibration curves can be represented by two different linear equations, which are valid at different sugar concentration ranges. The linear regression equations of Cu/Co/CoO/NGC are I (mA)= 20.2708E-5 C (μM) + 0.0809 (R^2 = 0.998) for C = 10-1,900 μM and I (mA) = 12.9759E-5·C (μM) + 0.2272 (R^2 = 0.999) for C = 1,900-9,300 μM. The limit of detection (LOD) is 0.2 μM while the sensitivities are 1035 and 663 μA mM^{-1} cm^{-2} for the two equations, respectively. The LOD was calculated using the following equation: LOD =3 SD/m,[22] where SD is the

standard deviation of the peak currents of the blank, and m is the slope of the calibration curves.

The respective values for Cu/Co/CoO/NGC, Cu/NGC, Co/CoO/NGC, R-Cu/Co/CoO/NGC, and O-Cu/Co/CoO/NGC are listed in Table 1. The current-concentration (I-C) linear fitting results of Cu/Co/CoO/GC electrode are shown in Figure S8 (b). The sensitivities, the LOD value, and the linear range of Cu/Co/CoO/GC for sugar were 177 and 137 μA mM^{-1} cm^{-2}, 63 μM, and 230-9,850 μM respectively. We can from the poor performances confirmed that the catalytically active M-Nx moieties (M=Cu and Co) in the mixture Cu/Co/CoO/NGC played the key catalytic role for glucose oxidation. We have also added some experiments of various glucose/fructose ratios (1:0 and 0:1) as shown in supporting information (Figure S10 and Table S3). Compared with three typical ratios of glucose/fructose (1:0, 1:1, and 0:1) by the Cu/Co/CoO/NGC sensor at the same conditions, there is no obvious difference in performances. In addition, the Cu/Co/CoO/NGC sensor displayed better detection performance for glucose and fructose compared with the other similar previous works listed in Table 2.

In real samples of wine and juice, some co-existing interfering species with glucose and fructose might affect the sensor response. The selectivity and anti-interference results are shown in Figure 6a. The interfering substances of 1 mM sucrose, 1 mM tartaric acid, 1 mM proline, 1 mM glycerine, 1 mM ethanol, 1 mM citric acid, and 1 mM ethyl acetate and could not disturb the current responses of 1 mM glucose, 1 mM fructose, and 1 mM glucose+ 1 mM fructose (1 mM glu+ 1 mM fru). Therefore, the advantage of the anti-interference ability fully confirms that the Cu/Co/CoO/NGC sensor has a high selectivity towards the non-enzymatic oxidation of glucose and fructose.

The reproducibility, repeatability and long-term stability of the Cu/Co/CoO/NGC sensor were evaluated in our work. Five Cu/Co/CoO/NGC electrodes were prepared independently and investigated by I-t tests in 0.2 M NaOH containing 1 mM and 5 mM sugar mixture solutions (equimolar concentration of glucose and fructose). The relative standard deviation (R.S.D.) was 5.2% and 7.3% (Table S4), respectively, indicating a high reproducibility of the prepared Cu/Co/CoO/NGC electrodes. For one Cu/Co/CoO/NGC modified electrode in five successive measurements, the R.S.D. was estimated to be 4.5% and 7.4% (Table S5) for the 1 mM and 5 mM of mixture

sugar solution, respectively. The good repeatability suggests that the Cu/Co/CoO/NGC sensor can be reused many times and is not easily affected by the oxidation products. The stability of Cu/Co/CoO/NGC was estimated by recording 50 consecutive CV curves in 0.2 M NaOH containing (or not) a 10 mM of mixed sugar solution (Figure 6b). The oxidation current did not change obviously during the 50 consecutive CV tests, implying the good stability of the Cu/Co/CoO/NGC sensor. The shelf life of the sensor was explored by comparing the performance of the freshly prepared sensor to those, stored for 2 or 4 weeks. The result (Figure S11) shows that the catalytic current responses remained at approximately 97.2% and 96.1% after 2 and 4 weeks, respectively. The good shelf life reflects the excellent antioxidation of the Cu/Co/CoO/NGC sample, which agrees with the previous conclusions.

Recently, screen-printed carbon electrodes (SPCEs) with versatility, low cost, miniaturized size, and easy connectivity to portable instruments have gained extensive attention from researchers and manufactures.[29] Disposable sensors based on SPCEs have led to many new possibilities in the detection of target analytes, such as DNA, biomolecules and glucose. Here, SPCEs modified with Cu/Co/CoO/NGC (Cu/Co/CoO/NGC/SPCEs) performed well towards the detection of sugar in a mixed solution, according to the CV and I-t tests (Figure 7a and 7b). The corresponding equations were I (mA)= 2.3516E-5 C (μM) + 0.0421 (R^2 = 0.995) and I (μA) = 1.0266E-5·C (μM) + 0.0658 (R^2 = 0.995). The limit of detection was 3.3 μM, the response time was 5 s, the linear range was C = 200-1,900 and 1,900-9,850 μM, and the sensitivity was 335 and 147 μA mM^{-1} cm^{-2} for the above two equations, respectively. Moreover, these data were obtained under the optimized concentration (20 mg mL^{-1}) of Cu/Co/CoO/NGC ink (Figure 7c). The concentration of 20 mg mL^{-1} was chosen because the too thick of dry modified material film of Cu/Co/CoO/NGC exhibited cracking and even peeling from the surface of the SPCEs when the concentration of the Cu/Co/CoO/NGC ink was greater than 20 mg mL^{-1}.

The potential application of the Cu/Co/CoO/NGC/SPCEs sensor was demonstrated by comparing it with the HPLC method for the detection of the sugar concentration in wine samples. When the I-t baseline was stable, 0.1 mL and 1 mL of wine were successively dropped into the stirred 0.2 M NaOH electrolyte, and the result is presented in Figure 7d. Table S6 lists the detection, the relative standard detection (R.S.D.), and the recovery performance compared to the HPLC method. The

R.S.D. and recovery were 1.7% and 103.2%, respectively. These good values suggest the high detection accuracy of Cu/Co/CoO/NGC/SPCEs in real samples.

4. Conclusion

In summary, nitrogen-doped graphic carbon (NGC)-coated Cu/Co/CoO nanoparticles (Cu/Co/CoO/NGC) were adopted to construct a sugar (glucose and fructose) sensor that achieved an excellent detection performance. The ultrasensitivity and high electrocatalytic activity are attributed to the synergistic effect between the Cu, Co and CoO nanoparticles coated by NGC and the catalytically active M-Nx moieties (M=Cu and Co). The intimate interaction between the NGC layers and the metallic nanoparticles accelerates the transmission of electrons between metal nanoparticles, and the NGC shells also improves the stability of the sensor in harsh conditions. Furthermore, the Cu/Co/CoO/NGC/SPCEs sensor (screen-printed carbon electrodes modified by Cu/Co/CoO/NGC) was used to detect the concentration of sugar (glucose and fructose) in wine and was compared with the HPLC technique to illustrate its good recovery and reliability. The inexpensive, rapid, and versatile characteristics of the modified SPCE sensor demonstrates its great potential in real sample detection in the near future.

Supporting Information

Supporting Information is available from the online or from the author.

Acknowledgements

This work was financially supported by the National Nature Science Foundation of China (No. 21576135), Jiangsu Natural Science Foundation for Distinguished Young Scholars (No. BK20170043), the Priority Academic Program Development of Jiangsu Higher Education Institutions, the Program for Changjiang Scholars, the Program for Jiangsu Specially-Appointed Professors, and the Youth Fund in Jiangsu Province (No. BK20150945).

Reference

[1] M. Thorpe, *China agr econ rev*, **1** (13), 301 (2016).

[2] T.R.I. Cataldi and D. Nardiello, *J. Agric. Food Chem.*, **51** (13), 3737 (2003).

[3] L.V. Shkotova, N.Y. Piechniakova, O.L. Kukla and S.V. Dzyadevych, *Food chemistry*, **197**, 972 (2016).

[4] J. Xu, N. Xu, X. Zhang, P. Xu, B. Gao, X. Peng, S. Mooni, Y. Li, J. Fu and K. Huo, *Sens Actuators B: Chem*, **244**, 38 (2017).

[5] J. He, J. Sunarso, Y. Zhu, Y. Zhong, J. Miao, W. Zhou, and Z. Shao, *Sens Actuators B: Chem*, **244**, 482 (2017).

[6] H. Zhu, L. Li, W. Zhou, Z. Shao and X. Chen, *J. Mater. Chem. B*, **5 (5)**, 1117 (2017).

[7] J.-S. Ye, C.-W. Chen and C.-L. Lee, *Sens Actuators B: Chem*, **208**, 569 (2015).

[8] H.-A. Chen, C.-L. Hsin, Y.-T. Huang, M. L. Tang, S. Dhuey, S. Cabrini, W.-W. Wu and S. R. Leone, *J. Phys. Chem. C*, **117** (43), 22211 (2013).

[9] L.C. Jiang and W.D. Zhang, *Biosen. Bioelectron*, **25** (6), 1402 (2010).

[10] Y. Liu, H. Jiang, Y. Zhu, X. Yang and C. Li, *J. Mater. Chem. A*, **4** (5), 1694 (2016).

[11] S.H. Noh, M.H. Seo, X. Ye, Y. Makinose, T. Okajima, N. Matsushita, B. Han and T. Ohsaka, *J. Mater. Chem. A*, **3** (44), 22031 (2015).

[12] B. Chen, F. Li, Z. Huang and G. Yuan, *Appl. Catal. B*, **200**, 192 (2017).

[13] J. Deng, D. Deng and X. Bao, *Adv Mater*, **29** (43), 1606967 (2017).

[14] H. Huo, C. Guo, G. Li, X. Han and C. Xu, *RSC Advances*, **4** (39), 20459 (2014).

[15] W. Ju, A. Bagger, G.P. Hao, A.S. Varela, I. Sinev, V. Bon, B. Roldan Cuenya, S. Kaskel, J. Rossmeisl and P. Strasser, *Nat. commun.*, **8**, 944 (2017).

[16] L. Wang, Y. Zheng, X. Lu, Z. Li, L. Sun and Y. Song, *Sens Actuators B: Chem*, **195**, 1 (2014).

[17] S.-J. Li, L.-L. Hou, B.-Q. Yuan, M.-Z. Chang, Y. Ma and J.-M. Du, *Microchim Act*, **183** (6), 1813 (2016).

[18] L. Bao, T. Li, S. Chen, C. Peng, L. Li, Q. Xu, Y. Chen, E. Ou and W. Xu, *Small*, **13** (5), 1602077 (2017).

[19] H. Obana, Motohik Hikuma, Takeo Yasuda, Isao Karube and S. Suzuki, *Ann NY Acad Sci*,**413** (1), 222 (1983).

[20] D. Xu, L. Luo, Y. Ding, L. Jiang, Y. Zhang, X. Ouyang and B. Liu, *J. Mater. Chem.*, **727**, 21 (2014).
[21] M. Busch, N.B. Halck, U.I. Kramm, S. Siahrostami, P. Krtil and J. Rossmeisl, *Nano Energy*, **29**, 126 (2016).
[22] J.I. Gowda and S.T. Nandibewoor, *Anal. Chem. Acta*, **7**, 539 (2015).
[23] Z.H. Ibupoto, K. Khun, V. Beni, X. Liu and M. Willander, *Sensors*, **13** (6), 7926 (2013).
[24] C. Hou, Q. Xu, L. Yin and X. Hu, *Analyst*, **137** (24), 5803 (2012).
[25] M. Li, C. Han, Y. Zhang, X. Bo and L. Guo, *Anal. Chem. Acta*, **861**, 25 (2015).
[26] D. Ye, G. Liang, H. Li, J. Luo, S. Zhang, H. Chen and J. Kong, *Talanta*, **116**, 223 (2013).
[27] Y.-W. Hsu, T.-K. Hsu, C.-L. Sun, Y.-T. Nien, N.-W. Pu and M.-D. Ger, *Electrochim. Acta*, **82**, 152 (2012).
[28] H. Liu, X. Lu, D. Xiao, M. Zhou, D. Xu, L. Sun and Y. Song, *Anal. Methods*, **5** (22), 6360 (2013).
[29] Z. Taleat, A. Khoshroo and M. Mazloum-Ardakani, *Microchim Acta*, **181** (9-10), 865-91 (2014).

Figure 1. (a) SEM image of Cu/Co/CoO/NGC; (b) TEM image of Cu/Co/CoO/NGC; (c) HRTEM image of Cu/Co/CoO/NGC

Figure 2. High-resolution N 1s XPS spectra of (a) Cu/Co/CoO/NGC, (b) Co/CoO/NGC, and (c) Cu/NGC; (d) N_2 adsorption-desorption isotherms of Cu/Co/CoO/NGC.

Figure 3. CV profiles for the Cu/Co/CoO/NGC, Cu/NGC and Co/CoO/NGC sensors in an Ar-saturated 0.2 M NaOH solution in the presence and absence of sugar (5 mM glucose and 5 mM fructose) at a 50 mV s^{-1} scan rate.

Figure 4. Catalytic reaction mechanism for glucose and the M-N_4 active site in alkaline electrolyte.

Figure 5. (a) Chronoamperometric responses (I-t) of Cu/Co/CoO/NGC, Co/CoO/NGC, and Cu/NGC electrodes in a 0.2 M NaOH solution with the successive addition of a sugar solution (the mixed sugar solution contains an equimolar concentration of glucose and fructose); the current-concentration (I-C) linear fitting results for (b) Cu/Co/CoO/NGC, (c) Co/CoO/NGC, and (d) Cu/NGC.

Figure 6. (a) Chronoamperometric responses (I-t) of the Cu/Co/CoO/NGC electrodes in the presence of interfering species; (b) 50 consecutive CV curves in Ar-saturated a 0.2 M NaOH solution with/without 5 mM glucose and 5 mM fructose.

Figure 7. (a) CV profiles for Cu/Co/CoO/NGC/SPCEs in an Ar-saturated 0.2 M NaOH solution in the presence and absence of 5 mM glucose and 5 mM fructose at a 50 mV s^{-1} scan rate. (b) The current-concentration (I-C) linear fitting results for Cu/Co/CoO/NGC/SPCEs. (c) The effect of the concentration of Cu/Co/CoO/NGC on the obtained anodic peak current; the insets show the CV tests in 5 mM glucose and 5 mM fructose containing 0.2 M NaOH electrolyte. (d) Chronoamperometric response (I-t) of the Cu/Co/CoO/NGC/SPCEs electrode in a 0.2 M NaOH solution at an applied potential of 0.4 V with the successive addition of wine: 0.1 mL wine and 1 mL wine.

Table 1. Sugar (glucose and fructose) detection performance for the Co/CoO/NGC, Cu/NGC, Cu/Co/CoO/NGC, and O-Cu/Co/CoO/NGC, and R-Cu/Co/CoO/NGC electrodes.

Samples	LOD (μM)	Response time (s)	Sensitivity ($\mu A\ mM^{-1}\ cm^{-2}$)	Linear regression equations
Co/CoO/NGC	1.01	4	310 (10-4,600 μM) 183 (4,600-13,150 μM)	y=6.0851E-5 x+0.0231 (R^2=0.998, 10-4,600 μM) y=3.5897E-5 x+0.1347 (R^2=0.997, 4,600-13,150 μM)
Cu/NGC	0.35	4	580 (10-1,900 μM) 320 (1,900-4,600 μM)	y=11.3893E-5 x + 0.03984 (R^2=0.996, 10-1,900 μM) y=6.293E-5 x + 0.1202 (R^2=0.992, 1,900-4,600 μM)
Cu/Co/CoO/NGC	0.22	3	1035 (10-1,900 μM) 663 (1,900-9,300 μM)	y=20.2708E-5 x+0.0809 (R^2=0.998, 10-1,900 μM) y=12.9759E-5 x+0.2272 (R^2=0.999, 1,900-9,300 μM)
O-Cu/Co/CoO/NGC	0.22	3	1028 (10-2,860 μM) 620 (2,860-9,859 μM)	y=20.1416E-5 x+0.0881 (R^2=0.998, 10-2,860 μM) y=12.1594E-5 x+0.3285 (R^2=0.997, 2,860-9,859 μM)
R-Cu/Co/CoO/NGC	0.56	4	420 (10-2,300 μM) 220 (2,300-9,300 μM)	y=8.1627E-5 x + 0.0443 (R^2=0.996, 10-2,300 μM) y=4.292E-5 x + 0.1192 (R^2=0.9952, 2,300-9,300 μM)

Table 2. Comparison of sugar (glucose and fructose) detection performance of the Cu/Co/CoO/NGC electrode to other related electrodes.

Modified electrodes	Sensitivity ($\mu A\ mM^{-1}\ cm^{-2}$)	LOD (μM)	Linear range (μM)	Stability (Recovery, %)	Reference
CuO NSs[a]	520	0.1	500-1,000	90(after 3 days)	[23]
Co_3O_4 NPs[b]	520.7	0.13	5-800	/	[24]
Co_3O_4-RGO	506.5	0.01	1000-6,500	64.9(after 1600s)	[25]
CuO-rGO-CNF	912.7	0.1	1-5,300	92(after 4 weeks)	[26]
CuOx-CoOx/graphene	507	0.5	5–570	92.6(after 4 weeks)	[17]
CuO-graphene	1065	1	1-5,300	92(after 2 weeks)	[27]
Cu-Co NSs[a]	1171	10	15-1,210	96.4(after 30 days)	[16]
3D Co_3O_4/graphene	122.16	0.157	Up to 80	93(after 5000 cycles of CV text)	[18]
Cu-Co–Ni NSs[a]	104.68	3.05	10-4,300	95.5(after 30 days)	[28]
Cu/Co/CoO/NGC	1035 (663)	0.2	10-9,300	96.1(after 4 weeks)	This work

[a] nanoparticles

[b] nanosheets

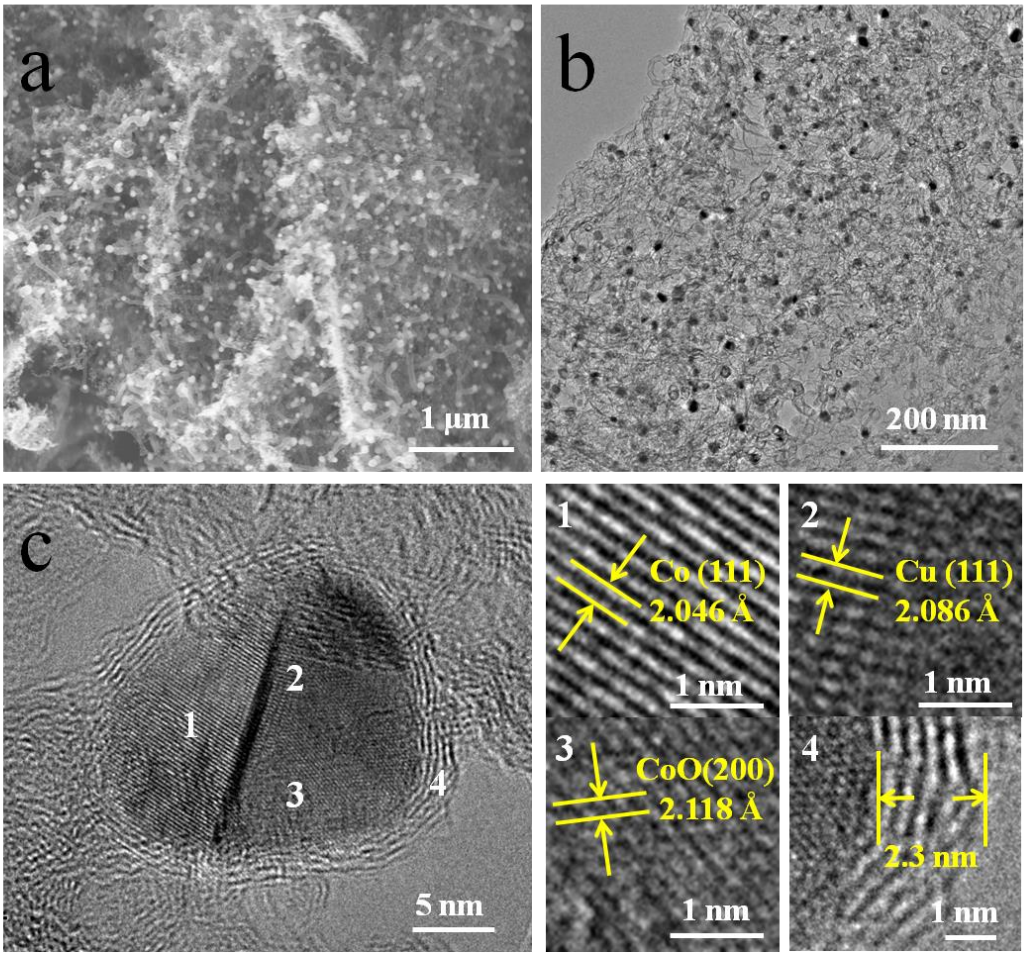
a
1 μm
b
200 nm
c
1
2
3
4
5 nm
1
Co (111)
2.046 Å
1 nm
2
Cu (111)
2.086 Å
1 nm
3
CoO(200)
2.118 Å
1 nm
4
2.3 nm
1 nm

Figure 1

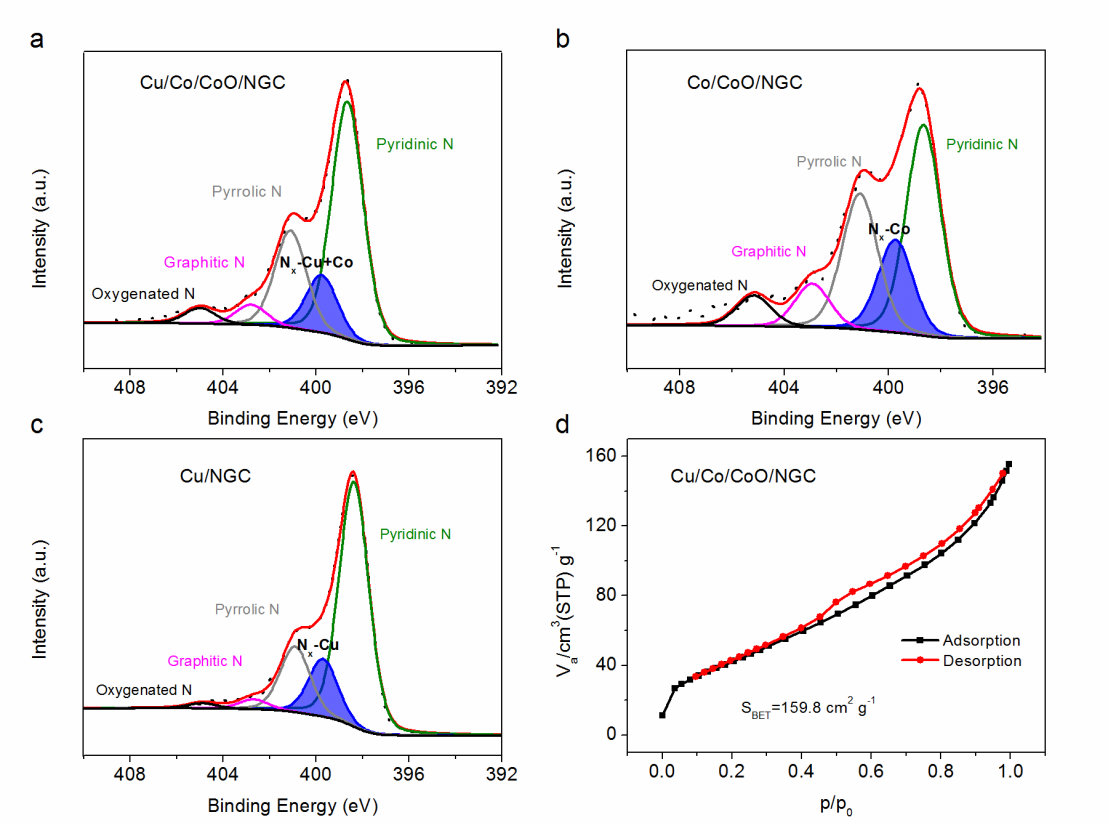
a
Cu/Co/CoO/NGC
Pyridinic N
Pyrrolic N
Graphitic N
N_x-Cu+Co
Oxygenated N
Intensity (a.u.)
408
404
400
396
392
Binding Energy (eV)
b
Co/CoO/NGC
Pyridinic N
Pyrrolic N
N_x-Co
Graphitic N
Oxygenated N
Intensity (a.u.)
408
404
400
396
Binding Energy (eV)
c
Cu/NGC
Pyridinic N
Pyrrolic N
N_x-Cu
Graphitic N
Oxygenated N
Intensity (a.u.)
408
404
400
396
392
Binding Energy (eV)
d
Cu/Co/CoO/NGC
Adsorption
Desorption
S_BET=159.8 cm^2 g^-1
V_a/cm^3(STP) g^-1
160
120
80
40
0
0.0
0.2
0.4
0.6
0.8
1.0
p/p_0

Figure 2

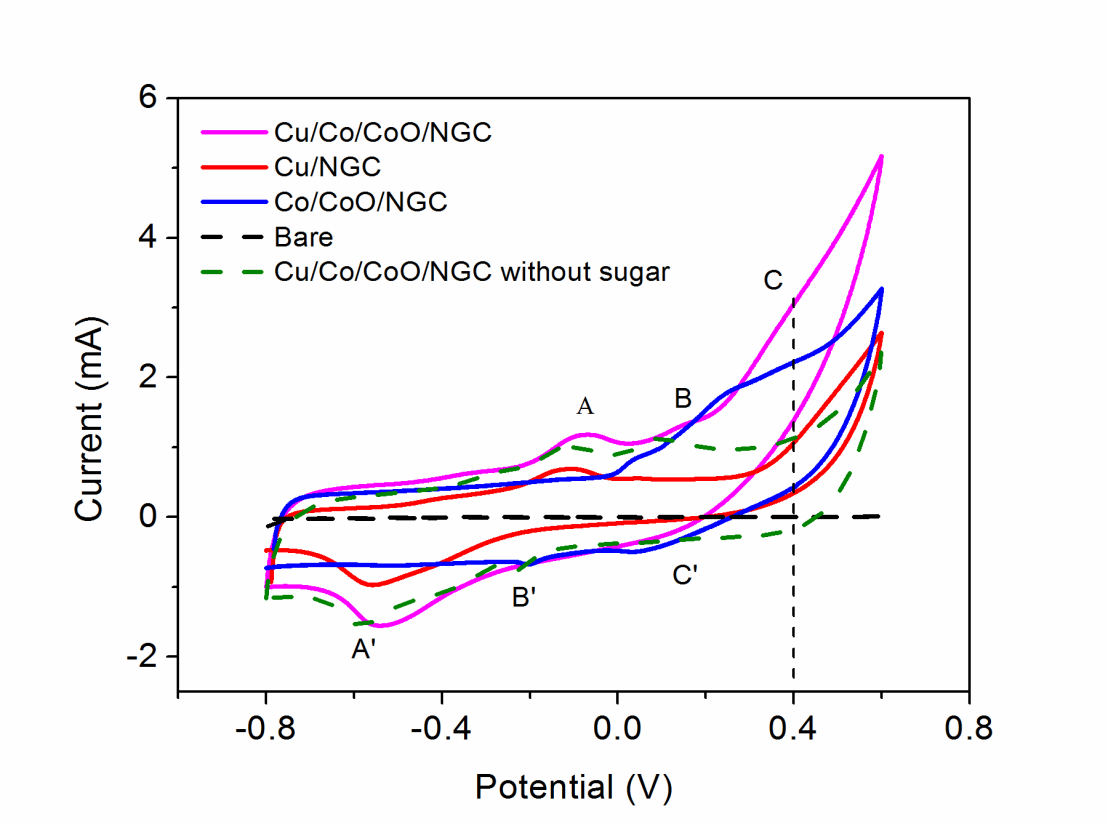

Figure 3

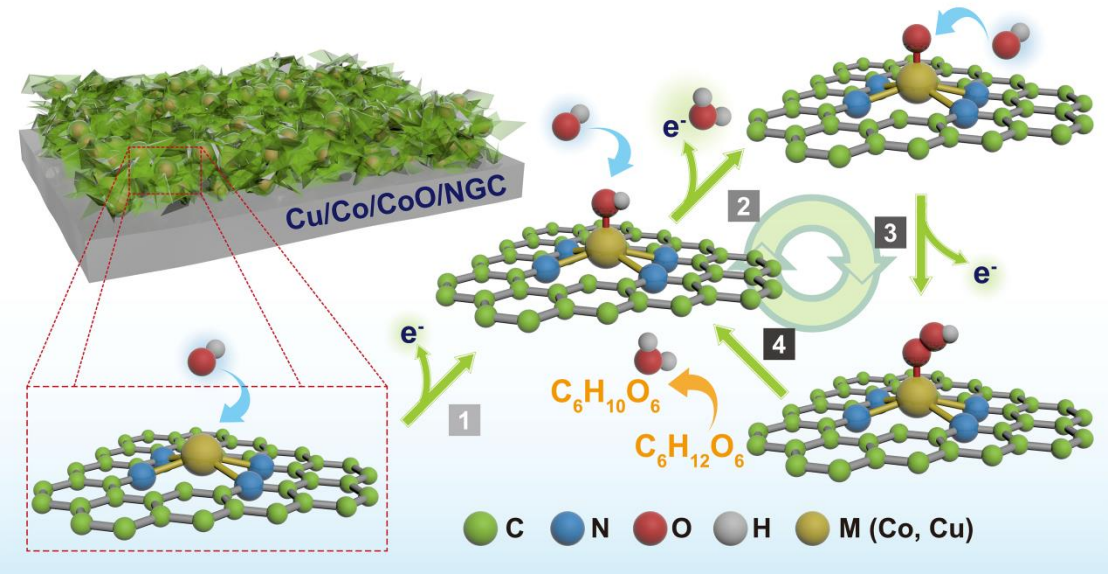

Figure 4

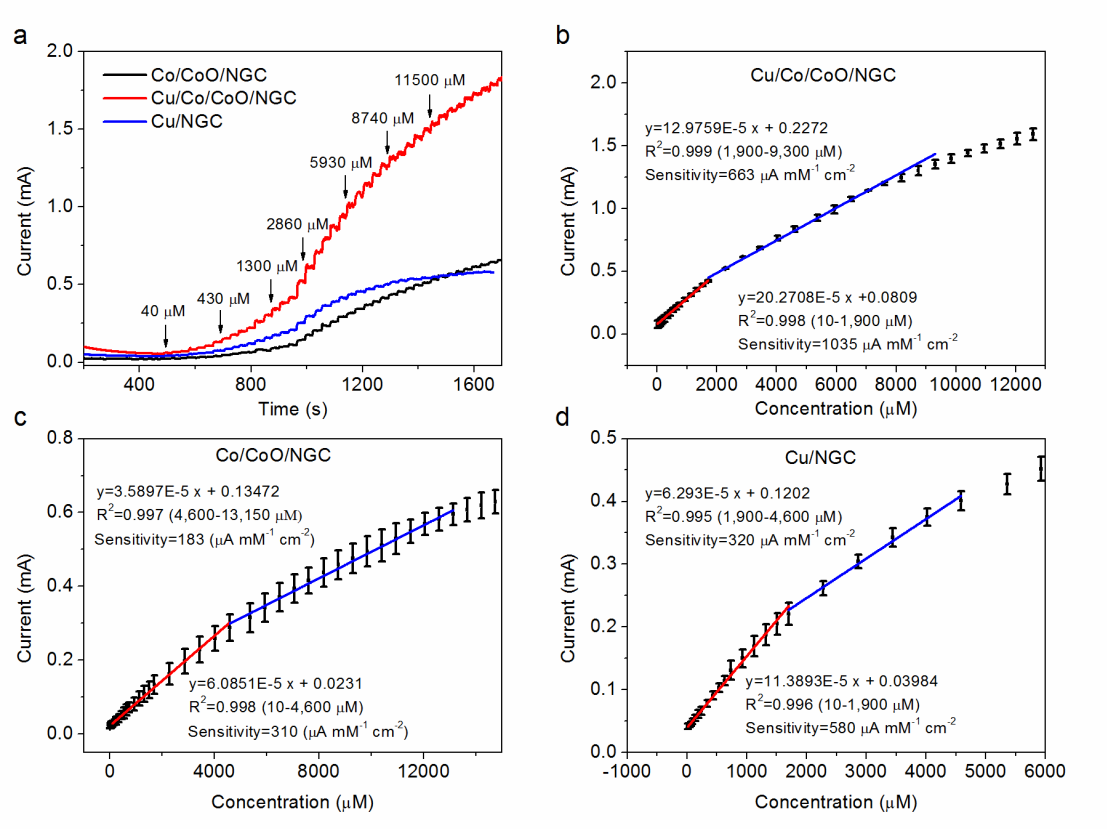

Figure 5

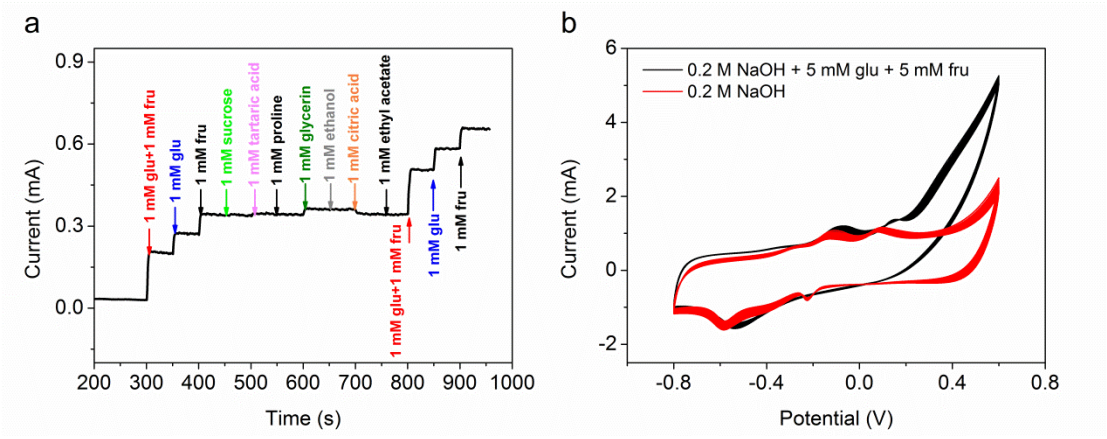

Figure 6

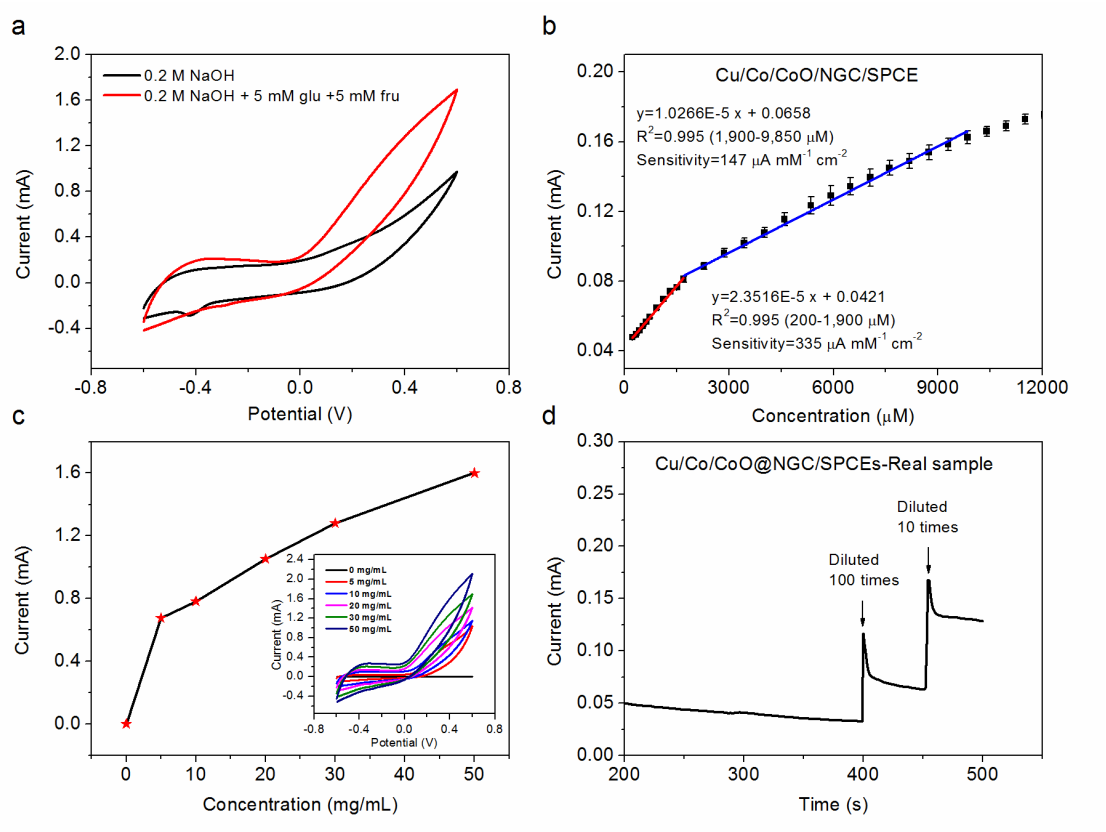
a
0.2 M NaOH
0.2 M NaOH + 5 mM glu +5 mM fru
Current (mA)
Potential (V)
b
Cu/Co/CoO/NGC/SPCE
y=1.0266E-5 x + 0.0658
R2=0.995 (1,900-9,850 μM)
Sensitivity=147 μA mM-1 cm-2
y=2.3516E-5 x + 0.0421
R2=0.995 (200-1,900 μM)
Sensitivity=335 μA mM-1 cm-2
Current (mA)
Concentration (μM)
c
Current (mA)
Concentration (mg/mL)
0 mg/mL
5 mg/mL
10 mg/mL
20 mg/mL
30 mg/mL
50 mg/mL
Current (mA)
Potential (V)
d
Cu/Co/CoO@NGC/SPCEs-Real sample
Diluted
10 times
Diluted
100 times
Current (mA)
Time (s)

Figure 7